



Article

Loranthus tanakae Franch. and Sav. Attenuates Respiratory Inflammation Caused by Asian Sand Dust

Se-Jin Lee ^{1,†}, So-Won Pak ^{1,†} , A Yeong Lee ^{2,3,4,†} , Woong-Il Kim ¹, Sung-Wook Chae ^{5,6}, Young-Kwon Cho ⁷, Je-Won Ko ⁸ , Tae-Won Kim ⁸ , Jong-Choon Kim ¹, Byeong Cheol Moon ² , Yun-Soo Seo ^{2,6,*} and In-Sik Shin ^{1,*}

- ¹ BK21 FOUR Program, College of Veterinary Medicine, Chonnam National University, 77 Yongbong-ro, Buk-gu, Gwangju 61186, Jeollanam-do, Republic of Korea; 218729@jnu.ac.kr (S.-J.L.); dvmpsw@jnu.ac.kr (S.-W.P.); dvmwoong@jnu.ac.kr (W.-I.K.); toxkim@jnu.ac.kr (J.-C.K.)
- ² Herbal Medicine Resources Research Center, Korea Institute of Oriental Medicine, 177 Geonjae-ro, Naju-si 58245, Jeollanam-do, Republic of Korea; lay7709@kiom.re.kr (A.Y.L.); bcmoon@kiom.re.kr (B.C.M.)
- ³ Department of Biotechnology, The Catholic University of Korea, 43 Jibong-ro, Wonmi-gu, Bucheon-si 14662, Gyeonggi-do, Republic of Korea
- ⁴ Department of Biomedical-Chemical Engineering, The Catholic University of Korea, 43 Jibong-ro, Wonmi-gu, Bucheon-si 14662, Gyeonggi-do, Republic of Korea
- ⁵ KM Convergence Research Division, Korea Institute of Oriental Medicine, 1672 Yuseong-daero, Yuseong-gu, Daejeon 34054, Chungcheongnam-do, Republic of Korea; sunguk.chae@kitox.re.kr
- ⁶ Center for Companion Animal New Drug Development, Jeonbuk Branch, Korea Institute of Toxicology (KIT), 30 Baekhak1-gil, Jeongeup-si 53212, Jeollabuk-do, Republic of Korea
- ⁷ College of Health Sciences, Cheongju University, 298 Daesung-ro, Sangdang-gu, Cheongju-si 28503, Chungbuk, Republic of Korea; petmen@cju.ac.kr
- ⁸ BK21 FOUR Program, College of Veterinary Medicine, Chungnam National University, 99 Daehak-ro, Daejeon 34134, Chungcheongnam-do, Republic of Korea; rheoda@cnu.ac.kr (J.-W.K.); taewonkim@cnu.ac.kr (T.-W.K.)
- * Correspondence: yunsoo.seo@kitox.re.kr (Y.-S.S.); dvmshin@jnu.ac.kr (I.-S.S.); Tel.: +82-63-570-8631 (Y.-S.S.); +82-62-530-2835 (I.-S.S.)
- † These authors contributed equally to this work.



Citation: Lee, S.-J.; Pak, S.-W.; Lee, A.Y.; Kim, W.-I.; Chae, S.-W.; Cho, Y.-K.; Ko, J.-W.; Kim, T.-W.; Kim, J.-C.; Moon, B.C.; et al. *Loranthus tanakae* Franch. and Sav. Attenuates Respiratory Inflammation Caused by Asian Sand Dust. *Antioxidants* **2024**, *13*, 419. <https://doi.org/10.3390/antiox13040419>

Academic Editor: Peter J. Barnes

Received: 23 February 2024

Revised: 18 March 2024

Accepted: 22 March 2024

Published: 29 March 2024



Copyright: © 2024 by the authors. Licensee MDPI, Basel, Switzerland. This article is an open access article distributed under the terms and conditions of the Creative Commons Attribution (CC BY) license (<https://creativecommons.org/licenses/by/4.0/>).

Abstract: Asian sand dust (ASD), generally produced in East Asia, including China, Japan, and Korea, directly leads to the development of pulmonary disease and exacerbates underlying pulmonary diseases. *Loranthus tanakae* Franch. and Sav. is a traditional herbal medicine applied to improve various inflammatory conditions. Here, we evaluated the curative properties of *L. tanakae* ethanol extract (LTE) against pulmonary inflammation caused by ASD. Additionally, to investigate the mechanism of action of LTE, we performed network pharmacological analysis. ASD was administrated on day 1, 3, and 5 by intranasal instillation, and LTE was orally administered for 6 days. Administration of LTE significantly decreased inflammatory cytokines and the number of inflammatory cells in bronchoalveolar lavage fluid, which was accompanied by a decrease in inflammatory cell accumulation in pulmonary tissue. Administration of LTE decreased the expression of cyclooxygenase2 and matrix metalloproteinase-9 in mice exposed to ASD with the decline in p65 phosphorylation. Additionally, administration of LTE significantly elevated hemeoxygenase (HO)-1 expression in the pulmonary tissue of mice exposed to ASD. These results were consistent with the data of network pharmacological analysis. This experiment showed that LTE attenuated pulmonary inflammation caused by ASD via inhibition of NF- κ B and elevation of HO-1. Therefore, LTE may have potential as a therapeutic agent to treat pulmonary inflammation caused by ASD.

Keywords: *Loranthus tanakae* Franch. and Sav.; Asian sand dust; airway inflammation; network pharmacology; NF- κ B; HO-1

1. Introduction

Asian sand dust (ASD) is considered as an important social problem that threatens human health due to its harmful components [1]. Generally, ASD is called yellow dust or

China dust and mainly occurs during spring and autumn in East Asia, including China, Japan, and Korea [2]. ASD originates from the deserts of Mongolia and China and affects East Asia due to the air current [3,4]. Furthermore, there are continuously elevated contents of particulate matters in ASD with increasing industrialization; thereby, ASD has led to disorders in various organs, such as the eyes, lung, and skin, and aggravated underlying respiratory diseases [5]. In particular, ASD induces airway inflammation via the release of inflammatory cytokines such as interleukin tumor necrosis factor (TNF)- α , (IL)-1 β , and IL-6, resulting in the infiltration of inflammatory cells into ASD-exposed lesions [6]. Furthermore, ASD exposure in patients with asthma or chronic obstructive pulmonary disease exacerbates the degrees of underlying diseases throughout the activation of the inflammatory process [7]. However, although the riskiness induced by ASD exposure is continuously elevated, there has been hardly any development of therapeutics to control the respiratory disorder caused by ASD exposure.

Loranthus tanakae Franch. and Sav. has been applied to treat inflammatory diseases, particularly inflammatory respiratory diseases, as a conventional herbal remedy in China, Japan, and Korea [8]. According to previous studies, *L. tanakae* possesses various pharmacological activities, such as anti-inflammatory, antioxidant, and anticancer properties, which are associated with its ingredients, including afzelin, quercitrin, and rhamnetin 3-O- α -rhamnoside [9,10]. Furthermore, *L. tanakae* effectively suppresses airway inflammation caused by exposure to cigarette smoke. These documents indicate that *L. tanakae* may have therapeutic potential to treat inflammatory pulmonary disease. Considering this evidence, we predict that *L. tanakae* may effectively suppress airway inflammation induced by ASD exposure.

Thus, we detected the ingredients of *L. tanakae* ethanol extract (LTE) by means of high-performance liquid chromatography (HPLC) and explored the curative properties of LTE on an ASD-induced pulmonary inflammation model. To investigate the mechanism of action of LTE, we analyzed specific protein expression according to the data from network pharmacological analysis.

2. Materials and Methods

2.1. Plant Material

The aerial parts of *L. tanakae* were obtained from a herbalist in Jeongseon, Gangwondo in South Korea (voucher specimen No. 2-16-0335). The plant material was the same as in our previous study [10]. The results of analysis of four components, including afzelin, quercitrin, rhamnocitrin 3-rhamnoside, and rhamnoside 3-rhamnoside, in LTE were described in a previous study [10].

2.2. Small Molecules and Potential Target Genes

The chemical profiles of the main components of *L. tanakae* and related genes have been described in our previous report [10]. Potential target genes related to “pneumonia” were searched using the GeneCards: Human Gene Database (<https://www.genecards.org/>, version 5.14, accessed on 14 April 2023). The corresponding target gene information was searched in the UniProt database (<https://www.uniprot.org/>, accessed on 14 April 2023). Potential target genes were selected according to the intersection of genes associated with small molecules and disease-linked genes [10].

2.3. Protein–Protein Interaction (PPI)

Various proteins have numerous reactions in the human body because there are many protein–protein interactions in the human body [11,12]. PPI analyses were performed using the STRING database (<https://string-db.org/>, version 11.5, accessed on 14 April 2023) with a medium confidence score (≥ 0.400). The PPI's topology was analyzed and visualized using Cytoscape version 3.7.2 (<https://cytoscape.org/>, accessed on 14 April 2023), with node colors of red (large nodes) and blue (small nodes) [13].

2.4. Signaling Pathway Analysis

Signaling pathway analyses were performed using the DAVID (The Database for Annotation, Visualization and Integrated Discovery; <https://david.ncifcrf.gov/>, accessed on 24 April 2023) and KEGG (Kyoto Encyclopedia of Genes and Genomes; <https://www.genome.jp/kegg/>, accessed on 25 April 2023).

2.5. Physicochemical Characterization of Asian Sand Dust

Asian sand dust (ASD) was obtained from Power Technology Inc. (Arden Hills, MN, USA) and consisted of 50% JIS Z8901 Class 8 (SiO₂, Al₂O₃, Fe₂O₃, MgO, CaO, TiO₂) and 50% natural SiO₂. The primary size, morphology, and purity of ASD were evaluated as previously described [2].

2.6. Experimental Animals and ASD Induced Airway Inflammation Model Protocol

The animal model was established as previously described [2]. The animals (male C57BL/6 mice, 6 weeks old, Samtako, Osan, Republic of Korea) were randomly divided into 4 groups as follows: control group (CON, PBS intranasal exposure + PBS oral administration), ASD group (ASD, ASD intranasal exposure + PBS oral administration), and LTE groups (LTE 50 and 100, ASD intranasal exposure + LTE 50 and 100 mg/kg oral administration, respectively). ASD intranasal exposure (40 mg/kg) was conducted on days 1, 3, and 5 under slight anesthesia. LTE was administered daily from days 1 to 6 by oral gavage before ASD exposure.

2.7. Analysis of Bronchoalveolar Lavage Fluid and Serum

The animals were sacrificed 48 h after the last ASD exposure, and tracheostomy was performed to collect bronchoalveolar lavage fluid (BALF) according to a previous study [10]. The supernatant of BALF was used to measure tumor necrosis factor (TNF)- α , interleukin (IL)-1 β , and IL-6 using ELISA kits (BD Biosciences, San Jose, CA, USA). The pellets of BALF were diluted with PBS and then used to count the inflammatory cells of BALF. The number of inflammatory cells in BALF was measured using Countess II (Thermo Fisher Scientific, San Diego, CA, USA). Additionally, to determine differential cell counts, the diluted pellets were attached to glass slides and then stained with Diff-Quik agent (Biozoa, Seoul, Republic of Korea). The numbers of eosinophils, lymphocytes, macrophages, and neutrophils were counted using a light microscope, and then the obtained ratios of differential cell counts were adjusted to the results of the total inflammatory cell counts.

2.8. Western Blot

To investigate the signaling pathway related to LTE treatment, the right lung was homogenized. Western blot was performed as previously described [14]. The primary antibodies were used as follows: p-p65 (dilution 1:1000, Cell signaling, Danvers, MA, USA), matrix-metalloproteinase 9 (MMP-9; dilution 1:1000, Cell signaling), cyclooxygenase 2 (COX2; dilution 1:1000, Abcam, Cambridge, UK), hemoxygenase-1 (HO-1; dilution 1:1000, cell signaling), and β -actin (dilution 1:1000, cell signaling). The secondary antibody (Thermo Fisher Scientific) was diluted 1:3000 and used. The density of each protein band was measured using ChemiDoc (Bio-Rad, Hercules, CA, USA).

2.9. Histological Examination of Pulmonary Tissue

After sampling BALF, pulmonary tissues were fixed, and then a paraffin block was prepared. The paraffin block was sectioned (4 μ m) and then stained with hematoxylin and eosin (Sigma-Aldrich, St. Louis, MO, USA). To explore the effects of LTE on the expression of HO-1, NF- κ B, Nrf2, and 8-OHdG in ASD-exposed pulmonary tissue, immunohistochemistry was conducted using a commercial kit (Vector Laboratories, Burlingame, CA, USA) as previously described [15]. The following primary antibodies were used: anti-rabbit p-p65 (dilution 1:200, Thermo Fisher Scientific), anti-rabbit HO-1 (dilution 1:200, Abcam), anti-mouse Nrf2 (dilution 1:200, Santa Cruz, CA, USA), and anti-mouse 8-OHdG (dilution 1:200,

Santa Cruz). Quantitative analysis of the pulmonary inflammation and density of protein band was conducted using IMT i-Solution (IMT i-Solution Inc., Vancouver, BC, Canada).

2.10. Measurement of Reactive Oxygen Species (ROS)

For ROS detection in BALF, a 2', 7'-dichlorodihydrofluorescein (DCF) ROS/RNS assay kit (ab238535, Abcam) was performed according to the protocol of manufacturer. For intracellular ROS levels, NCI-H292 cells (CRL-1848, ATCC, Manassas, VA, USA) were incubated in a humidified chamber at 37 °C with 5% CO₂ for 45 min with a 2', 7'-dichlorodihydrofluorescein diacetate. Fluorescence was determined at 485 nm excitation/535 nm emission.

2.11. Immunofluorescence in NCI-H292 Cells

Immunofluorescence was conducted as previously described [10]. The primary antibodies were used as follows: NF-κB (cell signaling), MMP-9 (Abcam), and HO-1 (Abcam). The representative images were obtained using a confocal laser scanning microscope (ZEISS, Dresden, Germany).

2.12. Statistical Analysis

Data are expressed as the means ± standard deviation (SD). Statistical evaluation was conducted using analysis of variance (ANOVA) with Dunnett's adjustment. The values of $p < 0.05$ and $p < 0.01$ were determined to be significant.

3. Results

3.1. Physicochemical Characterization of ASD

The morphology of ASD was mainly characterized by spherical shapes according to SEM (Figure 1A) and TEM (Figure 1B) analysis. ASD consisted of O 50.37%, Si 43.38%, Al 3.98%, Fe 1.88%, Ca 0.15%, Ti 0.13%, and Mg 0.11%.

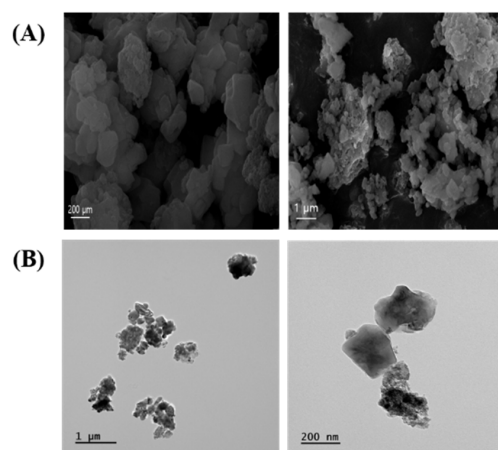


Figure 1. Morphology of ASD. (A) Morphology was measured by SEM. (B) Morphology was determined by TEM.

3.2. Potential Target Gene Analysis

In our previous report, there were a total of 173 genes associated with the main small molecules, which are rhamnetin 3-rhamnoside, rhamnocitrin 3-rhamnoside, quercetin 3-rhamnoside, and kaempferol 3-rhamnoside [10]. A total of 109 potential target genes were identified among 6755 pneumonia-related genes retrieved from GeneCards DB (Supplementary Table S1), for a total of 173 genes (Supplementary Table S2). A total of 33 genes were associated with 4 main small molecules, which were ACHE, ADORA1, ALDH2, ALOX5, CA2, CA4, CD38, CHEK1, CHEK2, COMT, DUSP3, EGN1, F10, HSP90AA1, IL2, NOX4, PDE5A, PIK3CA, PLG, PRKACA, PRKCA, PRKCB, PRKCD, PRKCE, PRKCZ, PTGS2, RAF1, RPS6KA3, SERPINE1, SLC29A1, TERT, TNF, and XDH. The potential gene network of small molecules was constructed with 113 nodes and 248 edges (Figure 2).

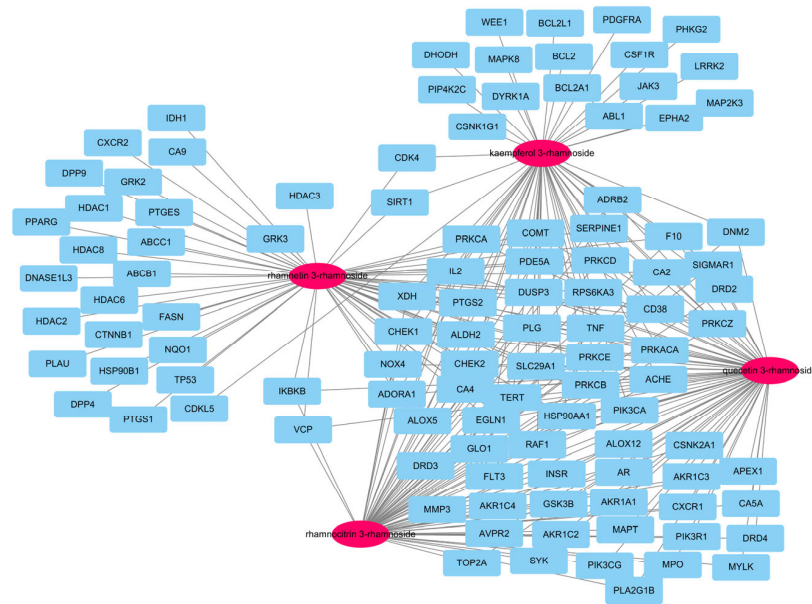


Figure 2. A network of 4 molecules (pink oval) and 109 potential target genes (blue rectangles). The network consisted of 113 nodes and 248 edges.

3.3. Protein-Protein Interaction (PPI)

The PPI network of 109 potential pneumonia-linked genes was constructed with 107 nodes and 722 edges. For network topology analysis, the top 10 degree genes were TP53, CTNNB1, TNF, HSP90AA1, PTGS2, SIRT1, PPARG, PIK3CA, BCL2L1, and IL2; the top 10 betweenness centrality genes were TP53, CTNNB1, TNF, HSP90AA1, PTGS2, PPARG, PRKACA, MAPT, NQO1, and AR; and the top 10 closeness centrality genes were TP53, CTNNB1, TNF, HSP90AA1, PTGS2, PPARG, SIRT1, BCL2L1, PIK3CA, and GSK3B. As a result of analyzing three factors in the PPI topology, it was confirmed that a total of six genes, TP53, CTNNB1, TNF, HSP90AA1, PTGS2, and PPARG, were core genes in this PPI network (Figure 3).

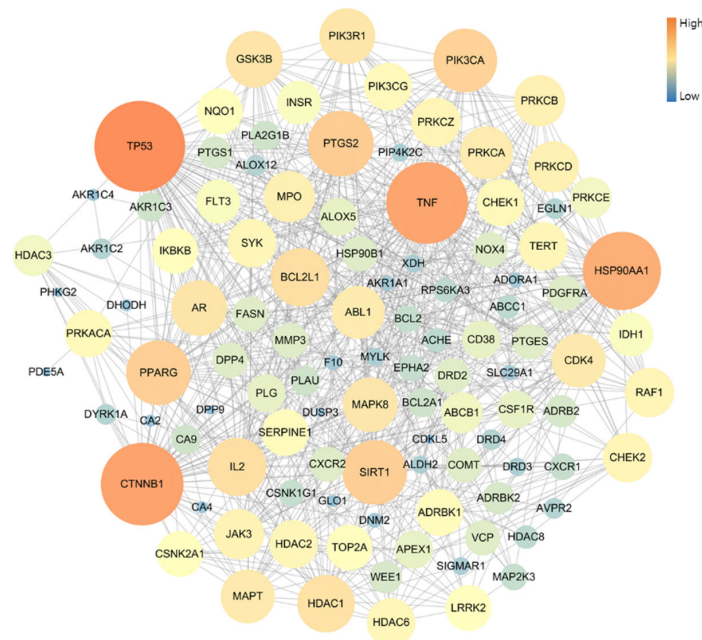


Figure 3. Topology analysis of PPI-associated pneumonia. The higher-degree genes are represented in large circles and orange color.

the production of IL-6 in comparison to the ASD group, which was detected in a dose-dependent manner. In addition, the production of TNF- α , IL-1 β , and -17 was obviously raised in the ASD group in comparison to the control group (Figure 6B,C,D, respectively). By contrast, the LTE-administered groups showed significant declines in TNF- α , IL-1 β , and -17 in comparison to the ASD group, which was obviously detected. ASD exposure remarkably raised the production of ROS in comparison to the control group (Figure 6E). But the LTE100 group showed a decline in the production of ROS in comparison to the ASD group.

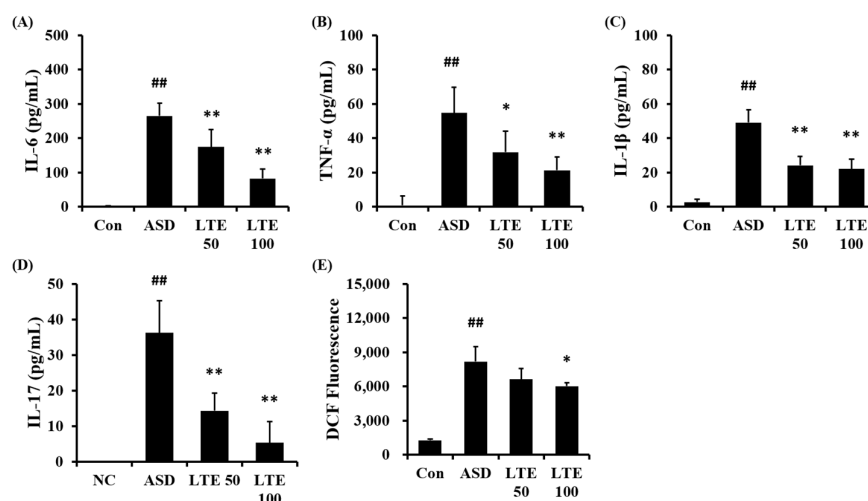


Figure 6. Effects of LTE on the production of inflammatory cytokines and ROS in mice exposed to ASD. (A) IL-6 level, (B) TNF- α level, (C) IL-1 β level, (D) IL-17 level, (E) ROS production. Con, PBS intranasal administration + PBS; ASD, ASD intranasal administration + PBS; LTE 50 and 100, ASD intranasal administration + LTE (50 and 100 mg/kg, respectively). The data are expressed as the mean \pm SD ($n = 5$). ##, $p < 0.01$, vs. Con; *, ** $p < 0.05$ and < 0.01 , vs. ASD, respectively.

3.7. Effects of LTE on Inflammatory Process of Pulmonary Tissue from Mice Exposed to ASD

ASD exposure caused extensive inflammatory responses in the pulmonary tissue in comparison to the control group (Figure 7A,B). However, the LTE-treated groups showed declines in the inflammatory process in pulmonary tissue compared with the ASD group, which was significantly observed in the LTE100 group.

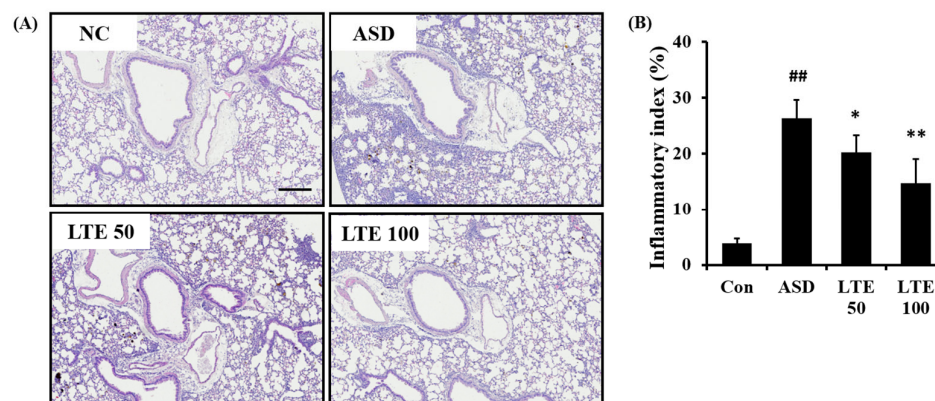


Figure 7. Effects of LTE on inflammatory responses of pulmonary tissue in mice exposed to ASD. (A) Representative figure for H&E-stained sections, (B) inflammatory index. Con, PBS intranasal administration + PBS; ASD, ASD intranasal administration + PBS; LTE 50 and 100, ASD intranasal administration + LTE (50 and 100 mg/kg, respectively). Scale bar indicates 100 μ m. The data are expressed as the mean \pm SD ($n = 5$). ##, $p < 0.01$, vs. Con; *, ** $p < 0.05$ and < 0.01 , vs. ASD, respectively.

3.8. Effects of LTE on Inflammatory Protein Expression in ASD Exposed Mice

ASD exposure induced the elevation of NF-κB expression in comparison to the control group (Figure 8A,B). By contrast, the LTE-administered groups showed decreased expression of NF-κB compared with the ASD group, which was obviously detected in the LTE100 group. The expression of MMP-9 and COX2 markedly increased with ASD exposure, which was reversed by LTE treatment. In addition, ASD exposure increased the HO-1 expression compared with the control group, and the LTE-administered groups had increased HO-1 expression compared to the ASD group. This was consistent with the results of ICH for pulmonary tissue. ASD exposure obviously increased the expression of NF-κB in pulmonary tissue in comparison to the control group (Figure 9A,B). By contrast, the LTE-administered groups showed meaningful declines in the expression of NF-κB in pulmonary tissue compared with the ASD group. In addition, the LTE-administered groups had elevated Nrf2 and HO-1 expression in pulmonary tissue compared with the ASD group, which was significantly observed in the LTE100 group (Figure 9A,C,D). The expression of 8-OHdG was elevated in the ASD group compared to the control group (Figure 9A). But the LTE-administered groups had remarkably decreased expression of 8-OHdG compared to the ASD group, which was obviously detected.

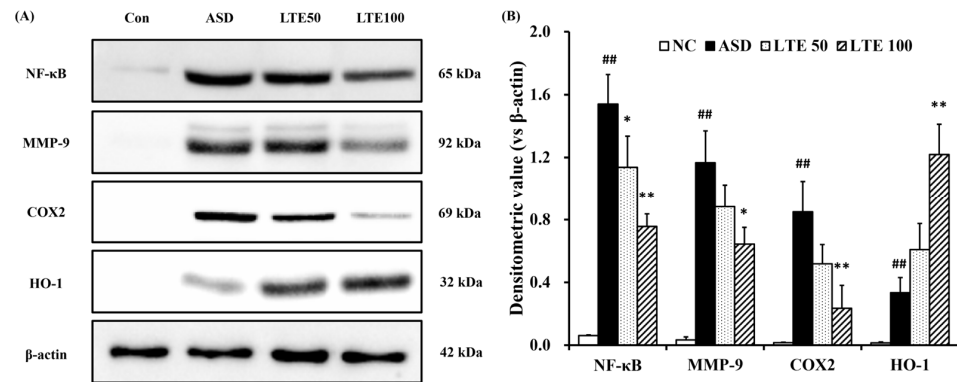


Figure 8. Effects of LTE on inflammatory protein expression in mice exposed to ASD. (A) Representative figure for protein expression, (B) densitometric value of protein expression. Con, PBS intranasal administration + PBS; ASD, ASD intranasal administration + PBS; LTE 50 and 100, ASD intranasal administration + LTE (50 and 100 mg/kg, respectively). The data are expressed as the mean ± SD ($n = 5$). ##, $p < 0.01$, vs. Con; *, ** $p < 0.05$ and < 0.01 , vs. ASD, respectively.

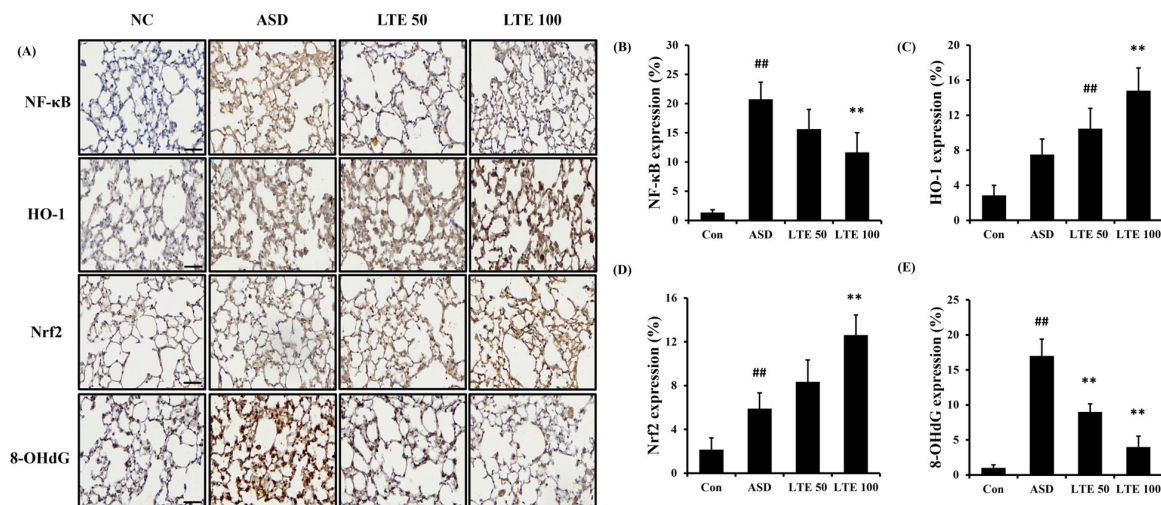


Figure 9. Effects of LTE on the expression of NF-κB, Nrf2, HO-1, and 8-OHdG in pulmonary tissue in mice exposed to ASD. (A) Representative figure for IHC, (B) NF-κB expression value, (C) Nrf2 expression

value, (D) HO-1 expression value, (E) 8-OHdG expression value. Con, PBS intranasal administration + PBS; ASD, ASD intranasal administration + PBS; LTE 50 and 100, ASD intranasal administration + LTE (50 and 100 mg/kg, respectively). Scale bar indicates 50 μ m. The data are expressed as the mean \pm SD ($n = 5$). ##, $p < 0.01$, vs. Con; ** $p < 0.01$, vs. ASD, respectively.

3.9. Effects of LTE on the ROS Production and Protein Expression in ASD-Stimulated NCI-H292 Cells

ASD exposure induced ROS generation in NCI-H292 cells, which was detected in a concentration-dependent manner (Figure 10A). Treatment of LTE and quercitrin effectively decreased the production of ROS induced by ASD exposure (Figure 10B,C). In addition, its translocation into the nuclei of ASD-stimulated cells was increased compared to that of non-stimulated cells (Figure 10D). By contrast, the LTE treatment groups had significantly decreased translocation of NF- κ B compared to ASD stimulated cells. Exposure to ASD induced the increased expression of HO-1 and MMP-9 compared to non-stimulated cells (Figure 10E). The expression of HO-1 was markedly increased compared to the ASD-stimulated cells. However, the expression of MMP-9 was decreased compared to the ASD-stimulated cells.

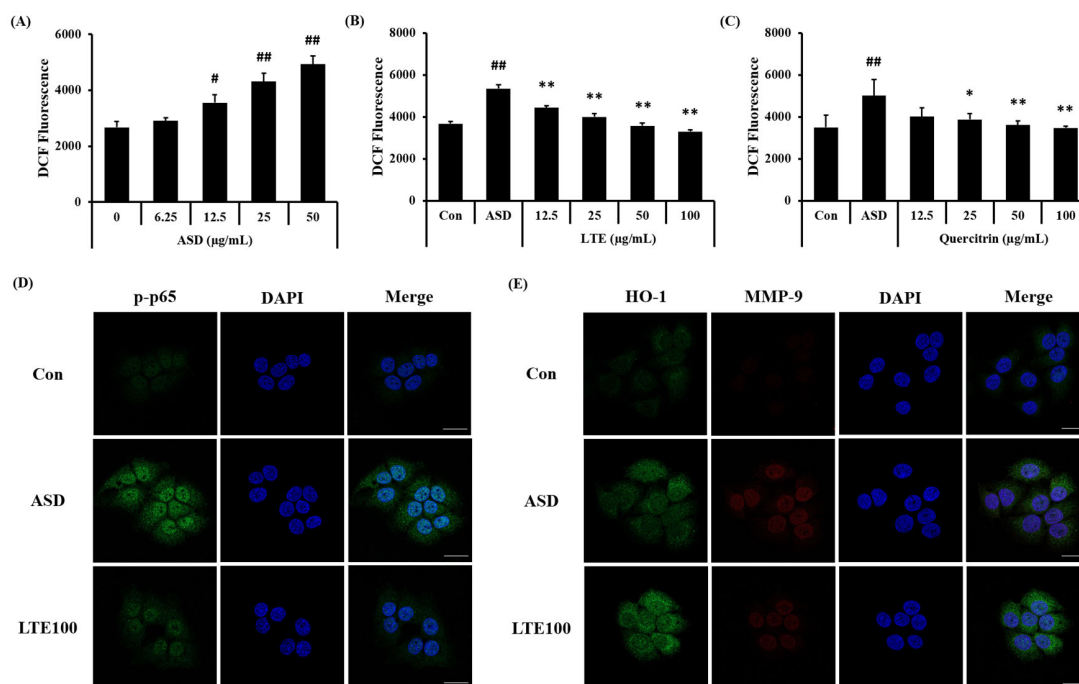


Figure 10. Effects of LTE and quercitrin on the ROS production and protein expression in ASD-stimulated NCI-H292 cells. ROS production in (A) ASD stimulated cells, (B) LTE-treated cells, and (C) quercitrin-treated cells. (D) Representative images for NF- κ B, (E) representative images for HO-1 and MMP-9. Scale bar = 20 μ m. The data are expressed as the mean \pm SD ($n = 3$). #, ##, $p < 0.05$ and 0.01, vs. Con, respectively; *, ** $p < 0.05$ and 0.01, vs. ASD, respectively.

4. Discussion

As industrialization accelerates, air pollution is emerging as a social problem. In particular, ASD, generated from Northeast Asia, contains various industrial substances, heavy metals, nanoparticles, and chemicals. It affects China, Korea, and Japan, and causes various respiratory diseases [3]. Here, we assessed the sanative effects of LTE in an ASD-exposed airway inflammation model and investigated its mechanism of action via network pharmacological analysis and protein assay. First, we analyzed four ingredients of LTE, including afzelin, quercitrin, rhamnocitrin 3-rhamnoside, and rhamnetin 3-rhamnoside. In an in vivo experiment, LTE treatment caused a significant decline in the inflammatory cell count and

inflammatory cytokines in BALF from mice exposed to ASD, along with decreases in inflammatory cell accumulation in pulmonary tissue. Furthermore, LTE treatment markedly decreased the protein expression, including NF- κ B, MMP-9, and COX2, related to the inflammatory process and elevated the HO-1 expression, acting as an antioxidant protein. This corresponded to the data of the network pharmacological analysis.

Because ASD consists of not only sand dust, but also various toxic stimuli, when exposed to the respiratory tract, it induces an extensive inflammatory response in the lung tissue [2]. In previous studies, ASD exposure has produced a significant amount of inflammatory cytokines, which induced inflammatory cell accumulation in pulmonary tissue and aggravated underlying respiratory diseases [6]. In this study, ASD exposure caused the elevation of inflammatory cytokines in BALF. But LTE treatment meaningfully decreased the production of inflammatory cytokines caused by ASD exposure, which was accompanied by declines in inflammatory cell count in BALF and airway inflammation in pulmonary tissue. Considering these results, LTE suppressed the pulmonary inflammation induced by ASD exposure.

Airway inflammation is a complex process involved in several signaling transduction. Particularly, NF- κ B is an important signaling pathway in inflammatory process [16]. It is activated by several stimuli, such as lipopolysaccharides, cytokines, and chemokines, which induce its phosphorylation with the activation of I κ B [17]. Then, translocation into the nucleus proceeds with the transcription of inflammatory associated genes, resulting in inflammatory cell infiltration into damaged lesions [18]. ASD exposure also acts as stimulus to activate NF- κ B, which induces airway inflammatory responses [19]. Therefore, the suppression of NF- κ B is considered as a crucial strategy to control ASD-induced airway inflammation. LTE administration markedly inhibited the expression of NF- κ B induced by ASD exposure, which was accompanied with a decline in the expression of COX2 and MMP-9. This indicates that the curative properties of LTE against ASD-related pulmonary inflammation are linked with the decrease in the expression of NF- κ B. Additionally, ASD exposure induced oxidative stress, which was involved in the alteration of harmful responses in the respiratory tract [6]. ASD exposure caused an imbalance of oxidants/antioxidants via the excessive production of ROS [20]. These events eventually induced a reduction in the antioxidant system, resulting in aggravated inflammation and apoptosis [21]. Therefore, several antioxidant systems exist to protect against oxidative stress. Of the antioxidant systems, HO-1 is an important molecule to reduce oxidative stress [22]. HO-1 is expressed via several irritations that cause ROS production and then diminish oxidative stress by catalyzing the degradation of heme to biliverdin/bilirubin, which act as antioxidants [23]. In a previous study, the overexpression of HO-1 induced a reduction in oxidative stress, but a deficiency of HO-1 caused an elevation of oxidative stress via excessive ROS production [24]. In the present study, LTE treatment markedly increased HO-1 expression compared with the ASD group. This indicates that LTE treatment effectively attenuated oxidative stress caused by ASD exposure.

LTE is a traditional herbal remedy in China, Japan, and Korea to control several inflammatory disorders. We detected four ingredients, including afzelin, quercitrin, rhamnocitrin 3-rhamnoside, and rhamnetin 3-rhamnoside, in LTE using an HPLC system. Four ingredients were associated with the therapeutic effects of LTE due to their pharmacological properties. Afzelin has antioxidative and anti-inflammatory properties and exerts suppressive effects against particulate matter-induced inflammatory skin diseases and ultraviolet radiation-induced damage [25,26]. Quercitrin has shown antioxidative and anti-inflammatory properties in various experiments, and is linked with the suppression of NF- κ B and overexpression of HO-1 [27]. Rhamnocitrin 3-rhamnoside and rhamnetin 3-rhamnoside showed strong antioxidant properties in our previous study [10]. Thus, our experiment is strongly supported by these previous studies.

In this study, PBS was used as a vehicle control. However, the solubility, stability, and bioavailability of LTE were not evaluated before using PBS as a vehicle control. Since these matters may affect the efficacy of the test material, it is considered essential to perform

animal experiment. If somewhat negative results occur regarding the pharmacological properties of test material, another vehicle control should be considered. These matters will need to be sufficiently reflected in further experiments.

Based on the data of network pharmacology analysis, the top 10 pathways (according to *p*-value) related to pneumonia were as follows: chemokine signaling, MAPK signaling, TNF signaling, FoxO signaling, Toll-like receptor signaling, autophagy-animal, VEGF signaling, NF- κ B signaling, mTOR signaling, and NOD-like receptor. Particularly, TNF and NF- κ B signaling may be linked in inflammatory processes. The signaling of TNF and NF- κ B stimulated by various irritation could lead to an inflammatory process via the production of inflammatory cytokines [28]. Additionally, TNF, FoxO, and NF- κ B were involved in pathological conditions associated with ROS generation. The signaling of TNF and NF- κ B could cause the progression of pulmonary inflammation due to excessive ROS generation [29]. On the other hand, FoxO signaling could activate antioxidant defense mechanisms such as HO-1, Nrf2, and superoxide dismutase to scavenge ROS [30]. Therefore, the curative properties of LTE against ASD-caused pulmonary inflammation may be linked with the elevation of HO-1 expression and inhibition of NF- κ B expression.

5. Conclusions

Overall, LTE treatment effectively attenuated pulmonary inflammatory process induced by ASD exposure, which was related to the elevation of HO-1 expression and inhibition of NF- κ B expression. Thus, LTE may be used as a potential therapeutic remedy for treating pulmonary inflammation.

Supplementary Materials: The following supporting information can be downloaded at: <https://www.mdpi.com/article/10.3390/antiox13040419/s1>, Table S1: Pneumonia-related genes in Gene Cards database; Table S2: Information of small molecules and genes in *Loranthus tanakae*.

Author Contributions: Conceptualization, I.-S.S. and Y.-S.S.; methodology, A.Y.L. and S.-J.L.; data curation, S.-W.P. and Y.-S.S.; formal analysis, A.Y.L., W.-I.K., S.-W.P., S.-J.L., S.-W.C., Y.-K.C., J.-W.K., T.-W.K., B.C.M. and Y.-S.S.; resources, A.Y.L.; project administration, S.-J.L.; investigation, S.-W.P.; writing—original draft preparation, S.-W.P., S.-J.L. and A.Y.L.; writing—review and editing, I.-S.S., Y.-S.S. and J.-C.K.; funding acquisition, Y.-S.S.; supervision, I.-S.S. All authors have read and agreed to the published version of the manuscript.

Funding: This work was supported by the national Research Foundation of Korea, granted by Korea Government (NRF-2020R1A4A1019395, NRF-2022R1A2C1010628 and RS-2023-00219517); the Development of Sustainable Application for Standard Herbal Resources (KSN2021320); and the Convergence Research Group project (CRC21021) of the National Research Council of Science and Technology.

Institutional Review Board Statement: The procedure used in this experiment was approved by the Institutional Animal Care and Use Committee of the Chonnam National University (CNU IACUC-YB-2022-114).

Informed Consent Statement: Not applicable.

Data Availability Statement: Data are contained within the article or Supplementary Material.

Conflicts of Interest: The authors declare no conflicts of interest.

References

1. Watanabe, M.; Noma, H.; Kurai, J.; Kato, K.; Sano, H. Association with ambient air pollutants and school absence due to sickness in schoolchildren. *Int. J. Environ. Res. Public Health* **2021**, *18*, 6631. [CrossRef]
2. Kim, W.I.; Lim, J.O.; Pak, S.W.; Lee, S.J.; Shin, I.S.; Moon, C.; Heo, J.D.; Kim, J.C. Exposure to China dust exacerbates testicular toxicity induced by cyclophosphamide in mice. *Toxicol. Res.* **2023**, *39*, 115–125. [CrossRef]
3. Hashizume, M.; Kim, Y.; Ng, C.S.F.; Chung, Y.; Madaniyazi, L.; Bell, M.L.; Guo, Y.L.; Kan, H.; Honda, Y.; Yi, S.M.; et al. Health effects of Asian dust: A systematic review and meta-analysis. *Environ. Health Perspect.* **2020**, *128*, 66001. [CrossRef]

4. Kim, H.J.; Song, J.Y.; Park, T.I.; Choi, W.S.; Kim, J.H.; Kwon, O.S.; Lee, J.Y. The effects of BRL-50481 on ovalbumine-induced asthmatic lung inflammation exacerbated by co-exposure to Asian sand dust in the murine model. *Arch. Pharm. Res.* **2022**, *45*, 51–62. [[CrossRef](#)] [[PubMed](#)]
5. Kim, K.; Kim, S.D.; Shin, T.H.; Bae, C.S.; Ahn, T.; Shin, S.S.; Kim, H.J.; Lee, C.M.; Suh, G.H. Respiratory and systemic toxicity of inhaled artificial Asian sand dust in pigs. *Life* **2021**, *11*, 25. [[CrossRef](#)] [[PubMed](#)]
6. Yang, H.W.; Park, J.H.; Shin, J.M.; Lee, H.M.; Park, I.H. Asian sand dust upregulates IL-6 and IL-8 via ROS, JNK, ERK, and CREB signaling in human nasal fibroblasts. *Am. J. Rhinol. Allergy* **2020**, *34*, 249–261. [[CrossRef](#)] [[PubMed](#)]
7. Nakao, M.; Yamauchi, K.; Mitsuma, S.; Odaira, T.; Obata, H.; Chijimatsu, Y.; Ishihara, Y. Associations of ambient air pollutant concentrations with respiratory symptoms and perceived health status in Japanese adults with and without chronic respiratory diseases: A panel study. *J. Prev. Med. Public Health* **2019**, *52*, 416–426. [[CrossRef](#)] [[PubMed](#)]
8. Joo, S.W.; Kim, H.G.; Oh, E.J.; Ko, J.H.; Lee, Y.G.; Kang, S.C.; Lee, D.Y.; Baek, N.I. Cyclofarnesane sesquiterpene glucoside from the whole plant of *Loranthus tanakae* and its cytotoxicity. *J. Appl. Biol. Chem.* **2019**, *62*, 7–10. [[CrossRef](#)]
9. Kim, Y.K.; Kim, Y.S.; Choi, S.U.; Ryu, S.Y. Isolation of flavonol rhamosides from *Loranthus tanakae* and cytotoxic effect of them on human tumor cell lines. *Arch. Pharm. Res.* **2004**, *27*, 44–47. [[CrossRef](#)]
10. Park, S.W.; Lee, A.Y.; Lim, J.O.; Lee, S.J.; Kim, W.I.; Yang, Y.G.; Kim, B.; Kim, J.S.; Chae, S.W.; Na, K.; et al. *Loranthus tanakae* Franch. & Sav. suppresses inflammatory response in cigarette smoke condensate exposed bronchial epithelial cells and mice. *Antioxidants* **2022**, *11*, 1885. [[CrossRef](#)]
11. Hu, R.F.; Sun, X.B. Design of new traditional Chinese medicine herbal formulae for treatment of type 2 diabetes mellitus based on network pharmacology. *Chin. J. Nat. Med.* **2017**, *15*, 436–441. [[CrossRef](#)]
12. Huang, X.-F.; Cheng, W.-B.; Jiang, Y.; Liu, Q.; Liu, X.-H.; Xu, W.-F.; Huang, H.-T. A network pharmacology-based strategy for predicting anti-inflammatory targets of ephedra in treating asthma. *Int. Immunopharmacol.* **2020**, *83*, 106423. [[CrossRef](#)]
13. Di Silvestre, D.; Vigani, G.; Mauri, P.; Hammadi, S.; Morandini, P.; Murgia, I. Network Topological Analysis for the Identification of Novel Hubs in Plant Nutrition. *Front. Plant Sci.* **2021**, *12*, 629013. [[CrossRef](#)]
14. Lim, J.O.; Kim, W.I.; Pak, S.W.; Lee, S.J.; Park, S.H.; Shin, I.S.; Kim, J.C. Toll-like receptor 4 is a key regulator of asthma exacerbation caused by aluminum oxide nanoparticles via regulation of NF- κ B phosphorylation. *J. Hazard. Mater.* **2023**, *448*, 130884. [[CrossRef](#)] [[PubMed](#)]
15. Jung, T.Y.; Lee, A.Y.; Song, J.H.; Lee, M.Y.; Lim, J.O.; Lee, S.J.; Ko, J.W.; Shin, N.R.; Kim, J.C.; Shin, I.S.; et al. *Scrophularia koraiensis* Nakai attenuates allergic airway inflammation via suppression of NF- κ B and enhancement of Nrf2/HO-1 signaling. *Antioxidants* **2020**, *9*, 99. [[CrossRef](#)]
16. Barnabei, L.; Laplantine, E.; Mbongo, W.; Rieux-Laucat, F.; Weil, R. NF- κ B: At the borders of autoimmunity and inflammation. *Front. Immunol.* **2021**, *12*, 716469. [[CrossRef](#)]
17. Liu, T.; Zhang, L.; Joo, D.; Sun, S.C. NF-kappaB signaling in inflammation. *Signal Transduct. Target. Ther.* **2017**, *2*, 17023–17032. [[CrossRef](#)]
18. Shih, V.F.; Tsui, R.; Caldwell, A.; Hoffmann, A. A single NFkappaB system for both canonical and non-canonical signaling. *Cell Res.* **2011**, *21*, 86–102. [[CrossRef](#)] [[PubMed](#)]
19. Song, Y.; Ichinose, T.; Morita, K.; Nakanishi, T.; Kanazawa, T.; Yoshida, Y. Asian sand dust causes subacute peripheral immune modification with NF- κ B activation. *Environ. Toxicol.* **2015**, *30*, 549–558. [[CrossRef](#)]
20. He, M.; Ichinose, T.; Yoshida, S.; Nishikawa, M.; Sun, G.; Shibamoto, T. Role of iron and oxidative stress in the exacerbation of allergic inflammation in murine lungs caused by urban particulate matter <2.5 μ m and desert dust. *J. Appl. Toxicol.* **2019**, *39*, 855–867. [[CrossRef](#)]
21. Zuo, L.; Wijegunawardana, D. Redox role of ROS and inflammation in pulmonary diseases. *Adv. Exp. Med. Biol.* **2021**, *1304*, 187–204. [[CrossRef](#)]
22. Campbell, N.F.; Fitzgerald, H.K.; Dunne, A. Regulation of inflammation by the antioxidant haem oxygenase 1. *Nat. Rev. Immunol.* **2021**, *21*, 411–425. [[CrossRef](#)]
23. Consoli, V.; Sorrenti, V.; Grosso, S.; Vanella, L. Heme oxygenase-1 signaling and redox homeostasis in physiopathological conditions. *Biomolecules* **2021**, *11*, 589. [[CrossRef](#)]
24. Wang, Y.; Yang, C.; Elsheikh, N.A.H.; Li, C.; Yang, F.; Wang, G.; Li, L. HO-1 reduces heat stress-induced apoptosis in bovine granulosa cells by suppressing oxidative stress. *Aging* **2019**, *11*, 5535–5547. [[CrossRef](#)] [[PubMed](#)]
25. Kim, J.H.; Kim, M.; Kim, J.M.; Lee, M.K.; Seo, S.J.; Park, K.Y. Afzelin suppresses proinflammatory responses in particulate matter-exposed human keratinocytes. *Int. J. Mol. Med.* **2019**, *43*, 2516–2522. [[CrossRef](#)]
26. Shin, S.W.; Jung, E.; Kim, S.; Kim, J.H.; Kim, E.G.; Lee, J.; Park, D. Antagonizing effects and mechanism of afzelin against UVB-induced cell damage. *PLoS ONE* **2013**, *8*, e61971. [[CrossRef](#)] [[PubMed](#)]
27. Chen, Q.; Wei, Y.; Zhao, Y.; Xie, X.; Kuang, N.; Wei, Y.; Wei, Y.; Yu, M.; Hu, T. Intervening effects and molecular mechanism of quercitrin on PCV2-induced histone acetylation, oxidative stress and inflammatory response in 3D4/2 cells. *Antioxidants* **2022**, *11*, 941. [[CrossRef](#)] [[PubMed](#)]
28. Laurindo, L.F.; Santos, A.R.O.D.; Carvalho, A.C.A.; Bechara, M.D.; Guiguer, E.L.; Goulart, R.A.; Vargas Sinatora, R.; Araujo, A.C.; Barbalho, S.M. Phytochemicals and regulation of NF- κ B in inflammatory bowel diseases: An overview of in vitro and in vivo effects. *Metabolites* **2023**, *13*, 96. [[CrossRef](#)]

29. Zhang, Y.; Liang, J.; Cao, N.; Gao, J.; Song, L.; Tang, X. Coal dust nanoparticles induced pulmonary fibrosis by promoting inflammation and epithelial-mesenchymal transition via the NF- κ B/NLRP3 pathway driven by IGF1/ROS-mediated AKT/GSK3 β signals. *Cell Death Discov.* **2022**, *8*, 500. [[CrossRef](#)]
30. Van der Horst, A.; Burgering, B.M. Stressing the role of FoxO proteins in lifespan and disease. *Nat. Rev. Mo. Cell Biol.* **2007**, *8*, 440–450. [[CrossRef](#)]

Disclaimer/Publisher’s Note: The statements, opinions and data contained in all publications are solely those of the individual author(s) and contributor(s) and not of MDPI and/or the editor(s). MDPI and/or the editor(s) disclaim responsibility for any injury to people or property resulting from any ideas, methods, instructions or products referred to in the content.